







Platelet C3G protects from liver fibrosis, while enhancing tumor growth through regulation of the immune response

Cristina Baquero^{1,2} , Minerva Iniesta-González^{1,2†}, Nerea Palao^{1,2†}, Cristina Fernández-Infante^{3,4}, Mateo Cueto-Remacha^{1,2}, Jaime Mancebo^{1,2}, Samuel de la Cámara-Fuentes⁵ , María Rodrigo-Faus^{1,2}, M Pilar Valdecantos^{6,7}, Angela M Valverde^{6,7}, Celia Sequera^{1,8}, Sara Manzano¹, Ángel M Cuesta^{1,2}, Alvaro Gutierrez-Uzquiza^{1,2} , Paloma Bragado^{1,2†} , Carmen Guerrero^{3,4,9*†}  and Almudena Porras^{1,2*†} 

¹ Departamento de Bioquímica y Biología Molecular, Facultad de Farmacia, Universidad Complutense de Madrid, Madrid, Spain

² Instituto de Investigación Sanitaria del Hospital Clínico San Carlos (IdISSC), Madrid, Spain

³ Instituto de Biología Molecular y Celular del Cáncer (IMBCC), Universidad de Salamanca-CSIC, Salamanca, Spain

⁴ Instituto de Investigación Biomédica de Salamanca (IBSAL), Salamanca, Spain

⁵ Unidad de Proteómica, Centro de Técnicas Biológicas, Universidad Complutense de Madrid, Madrid, Spain

⁶ Instituto de Investigaciones Biomédicas (IIBM) Alberto Sols-Morreale (CSIC-UAM), Madrid, Spain

⁷ Centro de Investigación Biomédica en Red de Diabetes y Enfermedades Metabólicas Asociadas (CIBERdem), Instituto de Salud Carlos III, Madrid, Spain

⁸ Aix Marseille Univ, CNRS, Inserm, Institut Paoli-Calmettes, Centre de Recherche en Cancérologie de Marseille (CRCM), Marseille, France

⁹ Departamento de Medicina, Universidad de Salamanca, Salamanca, Spain

*Correspondence to: A Porras, Departamento de Bioquímica y Biología Molecular, Facultad de Farmacia, UCM, Ciudad Universitaria, Madrid, Spain.

E-mail: maporras@ucm.es or C Guerrero, Centro de Investigación del Cáncer, Campus Unamuno s/n, Salamanca, Spain. E-mail: cguerrero@usal.es

†Equal contributions.

*Co-senior investigators.

Abstract

Primary liver cancer usually occurs in the context of chronic liver disease (CLD), in association with fibrosis. Platelets have emerged as important regulators of CLD and liver cancer, although their precise function and mechanism of action need to be clarified. C3G (RapGEF1) regulates platelet activation, adhesion, and secretion. Here we evaluate the role of platelet C3G in chemically induced fibrosis and liver cancer associated with fibrosis using genetically modified mouse models. We found that while overexpression of full-length C3G in platelets decreased liver fibrosis induced by chronic treatment with CCl₄, overexpressed C3G lacking the catalytic domain did not, although in both cases platelet recruitment to the liver was similar. In addition, C3G deletion in platelets (PF4–C3GKO mouse model) increased CCl₄-induced liver damage and hepatic fibrosis, reducing liver platelets and macrophages. Moreover, early liver immune response to CCl₄ was altered in PF4–C3GKO mice, with a remarkable lower activation of macrophages and increased monocyte-derived macrophages compared to WT mice. On the other hand, in response to DEN+CCl₄, PF4–C3G WT mice exhibited more and larger liver tumors than PF4–C3GKO mice, accompanied by the presence of more platelets, despite having less fibrosis in previous steps. Liver immune cell populations were also differentially regulated in PF4–C3GKO mice, highlighting the higher number of macrophages, likely with a pro-inflammatory phenotype, present in the liver in response to chronic DEN+CCl₄ treatment. Proteins upregulated or downregulated in platelet-rich plasma from PF4–C3GKO compared to WT mice might regulate the immune response and tumor development. In this regard, enrichment analyses using proteomic data showed changes in several proteins involved in platelet activation and immune response pathways. Additionally, the higher secretion of CD40L by PF4–C3GKO platelets could contribute to their antitumor effect. Therefore, platelet C3G presents antifibrotic and protumor effects in the liver, likely mediated by changes in the immune response.

© 2025 The Author(s). *The Journal of Pathology* published by John Wiley & Sons Ltd on behalf of The Pathological Society of Great Britain and Ireland.

Keywords: C3G (RapGEF1); platelet; liver fibrosis; liver cancer; immune response

Received 28 October 2024; Revised 29 November 2024; Accepted 9 January 2025

No conflicts of interest were declared.

Introduction

Chronic liver disease (CLD), a major global health problem, can lead to liver cancer, the sixth most

common cancer [1,2]. Fibrosis, a hallmark of CLD, can progress to cirrhosis, the main risk factor for the development of hepatocellular carcinoma (HCC), the most frequent liver cancer [2]. However, the causal

relationship between fibrosis and HCC development remains unclear [3].

Hepatic injury activates fibrogenesis, which involves extracellular matrix (ECM) secretion [4,5] and induces regeneration, which requires hepatocyte proliferation. However, when liver damage becomes chronic, hepatocyte proliferation is impaired, and hepatic progenitor/oval cells are activated and expanded as an alternative regeneration mechanism [4,6].

Liver fibrosis and HCC development are complex processes regulated by several signals such as growth factors (e.g. TGF- β), cytokines (e.g. IL-6), and chemokines (e.g. CCL2/5), arising from the interaction of different liver cell types, mainly hepatic stellate cells (HSCs), hepatocytes, Kupffer cells (KCs) (resident macrophages), and infiltrated immune cells [2,5,7,8]. HSCs and cancer-associated fibroblasts are the main ECM producers [3]. During chronic injury, HSCs become activated, transdifferentiate into myofibroblasts, express α -smooth muscle actin (α -SMA), and secrete ECM, mainly collagen type I and III, promoting fibrosis and chronic inflammation [4,9–11]. All this can contribute to maintaining hepatic fibrogenesis and/or liver repair, depending on the context.

In HCC, immune cells play a dual role depending on the context and timing [2]. A better prognosis is associated with the existence of immune infiltrates in HCC patients owing to the capacity of CD8⁺ cytotoxic T cells to kill cancer cells [12]. However, in metabolic dysfunction-associated steatohepatitis (MASH) [formerly nonalcoholic steatohepatitis (NASH)] mouse models, CD8⁺T cells showed a pro-inflammatory and protumorigenic role, facilitated by platelet-mediated recruitment [13].

Platelets are key players in fibrosis, CLD, and HCC. Under physiological conditions, platelets maintain liver homeostasis and vascular integrity and regulate the immune system [14,15]. In CLD, their function seems to be dual. Higher platelet levels correlate with less fibrosis in CLD patients [15] owing to the increased release of antifibrotic factors (e.g. HGF) and the decrease in TGF- β [16]. However, platelets also exacerbate local inflammation by recruiting different immune cells [13] and secrete pro-fibrotic factors such as TGF- β , PDGF, and CXCL4 (also named PF4) [14].

In HCC, as in other cancers [17], platelets can also have a dual function; thrombocytosis has been associated with worse overall survival [18,19] and thrombocytopenia with better outcomes of HCC patients [20]. As HCC promoters, platelets can induce hepatocyte proliferation [14], angiogenesis, and monocyte recruitment. Platelet releasates also facilitate a switch from monocytes to pro-tumoral macrophages, favoring HCC progression [15]. Platelets can also exert immunosuppressive effects through interaction with natural killer (NK) and T cells [14].

C3G (or RapGEF1) is a guanine nucleotide exchange factor (GEF) for Rap1 that regulates multiple cellular functions [21–24] through mechanisms dependent or independent of its GEF activity [25–27]. In cancer, C3G exerts different functions depending on tumor type and stage [23,28,29]. In HCC, C3G is upregulated [30]

and plays a dual role promoting tumor growth while inhibiting invasion.

C3G also induces megakaryocytic differentiation and pro-platelet formation [31] and regulates platelet biology [32–35]. Acting through Rap1b, C3G mediates signaling cascades triggered by several agonists to induce platelet activation, aggregation, and thrombus formation. C3G also regulates platelet α -granule release via Rap1-dependent and independent mechanisms, favoring angiogenesis and metastasis in melanoma and lung cancer models [35,36]. Based on C3G functions on platelets and the key role of platelets in liver fibrosis and HCC, we evaluated how platelet C3G regulates these processes using genetically modified mouse models. Our results suggest that platelet C3G protects from liver fibrosis, favors chemically induced tumor development, and regulates immune response to liver damage.

Materials and methods

Genetically modified mouse models

Transgenic mice overexpressing human full-length C3G (tgC3GFL) or C3G lacking the catalytic domain (tgC3G Δ Cat) in megakaryocytes and platelets and a conditional megakaryocyte/platelet C3G knockout (PF4-C3GKO) mouse, previously described and characterized [31–36], were used. Each transgenic and knockout mouse had a different WT control, which may show behavior differences since they have different genetic backgrounds.

Induction of liver fibrosis and HCC associated with fibrosis

Liver fibrosis was induced with CCl₄ [37] and HCC associated with fibrosis with DEN (diethylnitrosamine) and CCl₄ [38].

All animal experiments were carried out in compliance with the European Community Council Directive 2010/63/EU, following guidelines for animal research from Complutense University Ethical Committee and approved by Comunidad de Madrid (Spain) with references PROEX226.5/20 and PROEX176.0/24.

To analyze liver fibrosis, dewaxed liver paraffin sections were stained with Picro-Sirius Red.

Isolation and analysis of nonparenchymal liver cells by flow cytometry

Nonparenchymal cells (NPCs) were isolated as described previously [39,40].

Preparation of platelet-rich plasma, platelet stimulation with ADP, and secretome generation

Blood collected in EDTA-pretreated tubes was centrifuged twice at 100 \times *g* to obtain platelet-rich plasma (PRP). PRPs were centrifuged at 1300 \times *g* to isolate platelets, which were stimulated with ADP and

centrifuged at $2500 \times g$, collecting the supernatant with the secretome.

Isolation and stimulation of peritoneal macrophages

Mice were treated with 3% thioglycolate, and 4 days later the peritoneum fluid was aspirated to isolate macrophages. Cultured macrophages were stimulated with LPS or platelet secretomes.

Wide proteomic analysis

PRP protein extracts from PF4-C3GKO and WT mice treated with DEN+CCl₄ or the vehicle for 14 weeks were digested with trypsin and analyzed using nano-liquid chromatography coupled to a high-resolution mass spectrometer. Data were subjected to Gene Ontology (GO) enrichment [41] and additional analyses.

Statistical analysis

Data are represented as the mean \pm SEM ($n = 3$ –8 mice). Unpaired Student's *t*-test, one-way or two-way ANOVA, followed by Tukey or Bonferroni multiple-comparison tests were used. Differences were considered significant at $p \leq 0.05$. Additional details are provided in Supplementary materials and methods.

Results

Platelet C3G promotes platelet recruitment to the liver in response to CCl₄, protecting from fibrosis

Considering platelets' involvement in CLD, regulating fibrosis and liver cancer [14,15], and the important functions of C3G in platelets [32–36], we explored the role of platelet C3G in CCl₄-induced liver fibrosis using genetically modified mouse models.

Treatment of mice with CCl₄ for 4 weeks led to similar collagen accumulation in livers from mice overexpressing C3GFL (tgC3GFL) or C3GΔCat (tgC3GΔCat) in platelets and WT (supplementary material, Figure S1). However, after 8 weeks of treatment with CCl₄ less collagen was accumulated in livers from tgC3GFL compared to WT mice, while no differences between livers of tgC3GΔCat mice and their WT counterparts were found (Figure 1A and supplementary material, Figure S2A and Table S2). In contrast, in PF4-C3GKO mice treated with CCl₄ for 8 weeks, collagen accumulation in the liver was significantly higher than in WT animals (Figure 1A). Similarly, liver α -SMA levels, which increased in response to CCl₄ (8 weeks) in mice from all genotypes, were lower in tgC3GFL, reaching the highest levels in PF4-C3GKO mice (Figure 1B and supplementary material, Figure S2B), which resulted in an increased activity of alanine amino transferase (ALT) and aspartate amino transferase (AST), indicative of liver damage (supplementary material, Figure S3). This suggests that platelet C3G protects against liver fibrosis and chronic damage after CCl₄ treatment.

Next, we analyzed liver platelets. Figure 1C shows a higher number of platelets (CD41⁺) in livers from untreated tgC3GFL or tgC3GΔCat mice than in their WT counterparts. However, treatment with CCl₄ for 8 weeks only increased liver platelets in WT mice. In agreement with this, the number of liver platelets in PF4-C3GKO mice did not increase in response to CCl₄, remaining lower than in WT animals. This indicates that platelet C3G overexpression promotes platelet recruitment to the liver, even in untreated mice, while deletion of C3G in platelets prevents this recruitment in response to CCl₄.

Macrophages contribute to HSC activation and progression of liver fibrosis [42]. Therefore, we quantified liver macrophages (F4/80+). Untreated tgC3GFL and tgC3GΔCat mice had more liver macrophages (Figure 1D), which decreased upon treatment with CCl₄ for 8 weeks in tgC3GFL mice, remaining unchanged in tgC3GΔCat animals. Moreover, the increase in liver macrophages induced by CCl₄ in WT mice was impaired in PF4-C3GKO animals. All this suggests that the number of liver macrophages is regulated by platelet C3G.

A variety of liver cell types, recruited immune cells, and platelets can secrete growth factors, cytokines, and chemokines that regulate liver fibrosis. Thus, we evaluated the liver expression of some of them after 4 and 8 weeks of treatment with CCl₄. *Hgf* mRNA was increased in livers from untreated tgC3GFL compared to WT mice at 4 weeks, showing a tendency to decrease upon CCl₄ treatment. However, no changes were found in tgC3GΔCat mice (supplementary material, Figure S4). Curiously, *Il6* mRNA levels were upregulated in livers from untreated tgC3GFL and tgC3GΔCat mice, and *Il1b* mRNA was more expressed in livers from untreated tgC3GΔCat mice, decreasing after CCl₄ treatment for 4 weeks (supplementary material, Figure S4). After 8 weeks of treatment with CCl₄ no significant differences in their expression between genotypes were found, except for the increase in *Il6* mRNA detected in livers from tgC3GFL mice (supplementary material, Figure S5). Additionally, *Hgf* mRNA expression was reduced in PF4-C3GKO livers, increasing upon CCl₄ treatment (8 weeks). Since changes in these mRNAs were not significant in most cases, we determined IL-1 β , IL-6, and CCL2 protein levels in the liver under these conditions. IL-1 β protein levels decreased in livers from tgC3GFL mice compared to their WT counterparts, while pro-IL-1 β remained unchanged. IL-6 levels increased in livers from tgC3GFL mice treated with CCl₄ and in untreated C3GΔCat mice compared with their corresponding WT counterparts, while a reduction was observed in PF4-C3GKO mice (Figure 2A and supplementary material, Figure S6). No changes between genotypes were observed in CCL2 in response to CCl₄.

Platelet C3G regulates early liver immune response to CCl₄, increasing macrophage activation

Although platelet C3G seems to protect against liver fibrosis induced by CCl₄, we only detected limited changes in the expression of potential regulatory factors

at either 4 or 8 weeks when comparing the different genotypes. Early changes in cytokines and chemokines (e.g. CXCL4) and the subsequent platelet recruitment are important to induce fibrosis and to recruit immune cells to the liver upon CCl₄ treatment [43]. Hence, we studied the acute response to CCl₄, determining the

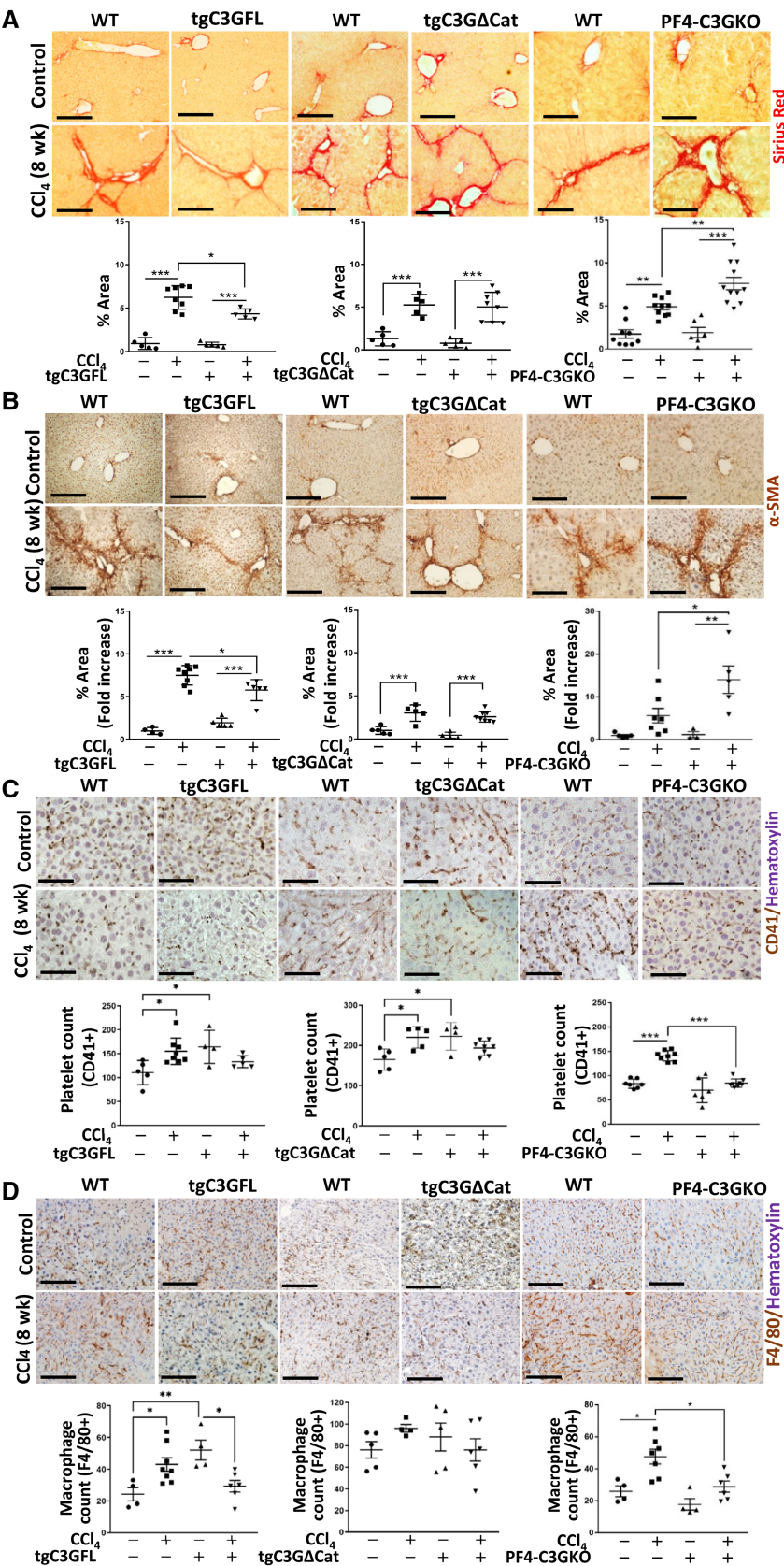


Figure 1 Legend on next page.

expression of IL-6, IL-1 β , CCL2, and CXCL4 following short-term treatment (24 h) with CCl₄ in mice from all genotypes. With this brief CCl₄ treatment, *Il6* mRNA levels were only significantly increased in livers from PF4-C3GKO compared to WT mice, and CCl₄-induced *Il1b* mRNA expression was enhanced in tgC3GFL mice (Figure 2B). *Ccl2* mRNA expression was also accentuated in livers from tgC3GFL and PF4-C3GKO mice treated with CCl₄, while no differences between genotypes were observed in *Cxcl4* (Figure 2B). In most cases, the expression of these cytokines was similar in WT and tgC3G Δ Cat mice in response to CCl₄ (Figure 2B). Moreover, the analysis of IL-6, IL-1 β , and CCL2 protein levels under these conditions only revealed changes in IL-6 (Figure 2C and supplementary material, Figure S7). IL-6 levels increased more in livers from tgC3GFL mice treated with CCl₄ (24 h) compared to WT mice, although in all genotypes a rise was observed (Figure 2C and supplementary material, Figure S7).

Early changes in the immune cell populations induced by cytokines and other regulatory signals, some of them secreted by platelets, are relevant for chronic liver damage response [2,13,40]. Therefore, based on genotype-dependent differences in the number of liver macrophages after chronic CCl₄ treatment (Figure 1D), liver macrophages and platelets and serum ALT and AST activities were analyzed after CCl₄ treatment for 24 h. Whereas the increase in serum ALT and AST activities induced by CCl₄ was similar in tgC3GFL and tgC3G Δ Cat compared to their WT mice, AST activity was higher in PF4-C3GKO than in WT mice (supplementary material, Figure S8A). However, CCl₄ induced a similar recruitment of platelets to the liver in all genotypes (supplementary material, Figure S8B), and liver macrophages remained unchanged or tended to decrease regardless of genotype (supplementary material, Figure S8C). Therefore, to further understand the behavior of immune cells, a detailed analysis of immune cells was performed after 48 h of CCl₄ treatment only in PF4-C3GKO mice and their corresponding WT counterparts. Upon CCl₄ treatment for 48 h, the number of active macrophages only increased in the liver of WT mice (Figure 3A), while early recruited monocytes increased in PF4-C3GKO mice. On the other hand, monocyte-derived macrophages increased in the liver of both WT and PF4-C3G-KO mice treated with CCl₄ for 48 h, reaching higher levels in PF4-C3GKO mice.

Additionally, the number of lymphocytes and, specifically, helper T lymphocytes decreased after CCl₄ treatment for 48 h only in WT mice (Figure 3A). In contrast, cytotoxic lymphocytes did not change under any condition or genotype (Figure 3A). On the other hand, the number of neutrophils was higher in the liver of untreated WT animals compared to PF4-C3GKO mice and decreased after CCl₄ treatment for 48 h only in WT mice. However, the number of cytotoxic NK cells was significantly higher in livers from untreated PF4-C3GKO mice, decreasing upon CCl₄ treatment, while increasing in WT mice (Figure 3A); whereas the number of helper NK cells decreased after CCl₄ treatment only in WT mice. Therefore, the CD4+/CD8+ NKT ratio increased in livers from PF4-C3GKO mice treated with CCl₄ for 48 h.

All these data indicate that the early immune response to CCl₄ is altered in the liver of mice lacking C3G in platelets, with remarkable reduced macrophage activation and enhanced monocyte/macrophage recruitment.

To better understand how platelet C3G regulates macrophage phenotypes, isolated macrophages were stimulated with secretomes from ADP-activated WT and PF4-C3GKO platelets or LPS, an inducer of a pro-inflammatory phenotype. As expected, *Nos2* mRNA (encoding iNOS) was markedly induced by LPS and, to a lesser extent, by platelet secretomes, reaching higher levels with PF4-C3GKO-derived secretomes (Figure 3B). In addition, *Arg1* mRNA expression (anti-inflammatory phenotype marker) tended to be higher upon stimulation with secretomes from WT platelets, and *Cd163* mRNA (anti-inflammatory phenotype marker) levels remained unchanged in all conditions (Figure 3B). These data suggest that PF4-C3GKO platelets secrete factors that may favor a pro-inflammatory macrophage phenotype.

Deletion of C3G in platelets exacerbates liver fibrosis while restraining hepatocarcinoma development induced by treatment with DEN plus CCl₄

Since platelet C3G seems to protect from liver fibrosis, we evaluated its function in a model of HCC associated with fibrosis induced by treatment with DEN and CCl₄ using PF4-C3GKO mice.

CCl₄ and DEN+CCl₄ induced a significantly higher collagen accumulation in livers from PF4-C3GKO compared to WT mice at 8 weeks (Figures 1A, 4A and supplementary material, Table S3). DEN+CCl₄ also

Figure 1. Platelet C3G increases platelet recruitment to the liver and liver macrophages, reducing fibrosis. Mice overexpressing full-length C3G (tgC3GFL) or C3G lacking the catalytic domain (tgC3G Δ Cat), as well as those lacking C3G (PF4-C3GKO) in megakaryocytes and platelets and their corresponding WT counterparts, were treated with CCl₄ or vehicle (controls) for indicated times. (A) Analysis of collagen accumulation assessed using Picro-Sirius Red staining in liver sections. Upper panels: representative microscope images; lower panels: graphics showing quantification of positive areas (percentage) for each sample and mean values \pm SEM. (B) Analysis of α -SMA levels in liver sections. Upper panels: representative microscope images; lower panels: graphics showing quantification of α -SMA-positive areas (percentage) for each sample and mean values \pm SEM. (C) Immunohistochemical analysis of liver platelets detected with CD41 antibody. Upper panels: representative microscope images; lower panels: graphics showing number of CD41-positive cells/field for each condition and mean values \pm SEM. (D) Immunohistochemical analysis of liver macrophages detected with F4/80 antibody. Upper panels: representative microscope images; lower panels: graphics showing number of F4/80 positive cells/field for each condition and mean values \pm SEM. * p \leq 0.05, ** p \leq 0.01, and *** p \leq 0.001 compared as indicated (n = 4–8). Scale bars: 20 μ m.

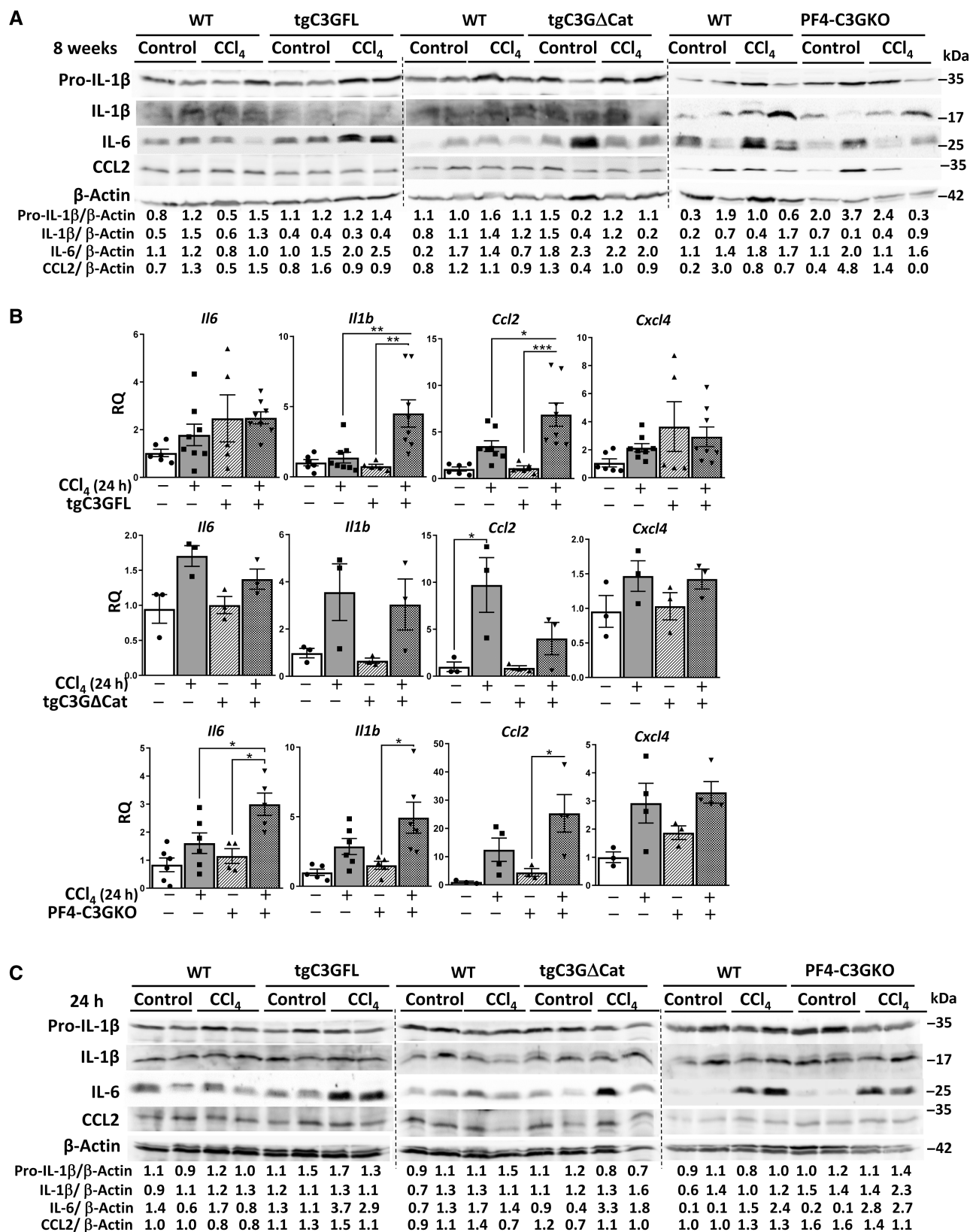


Figure 2. Regulation of expression of cytokines and chemokines by platelet C3G in response to chronic and acute treatment with CCl₄. Mice overexpressing full-length C3G (tgC3GFL) or C3G lacking catalytic domain (tgC3GΔCat), as well as those lacking C3G (PF4-C3GKO) in megakaryocytes and platelets and their corresponding WT counterparts, were treated with CCl₄ or vehicle (controls) for indicated times. (A and C) Western-blot analysis of IL-1β (pro-form and mature IL-1β), IL-6, and CCL2 in liver extracts normalized with β-actin. (B) RT-qPCR analysis of *Il6*, *Il1b*, *Ccl2*, and *Cxcl4* mRNA levels in liver samples. Histograms showing relative quantification (RQ) mean values ± SEM and individual values of each sample. **p* ≤ 0.05, ***p* ≤ 0.01, and ****p* ≤ 0.001 compared as indicated (*n* = 3–8).

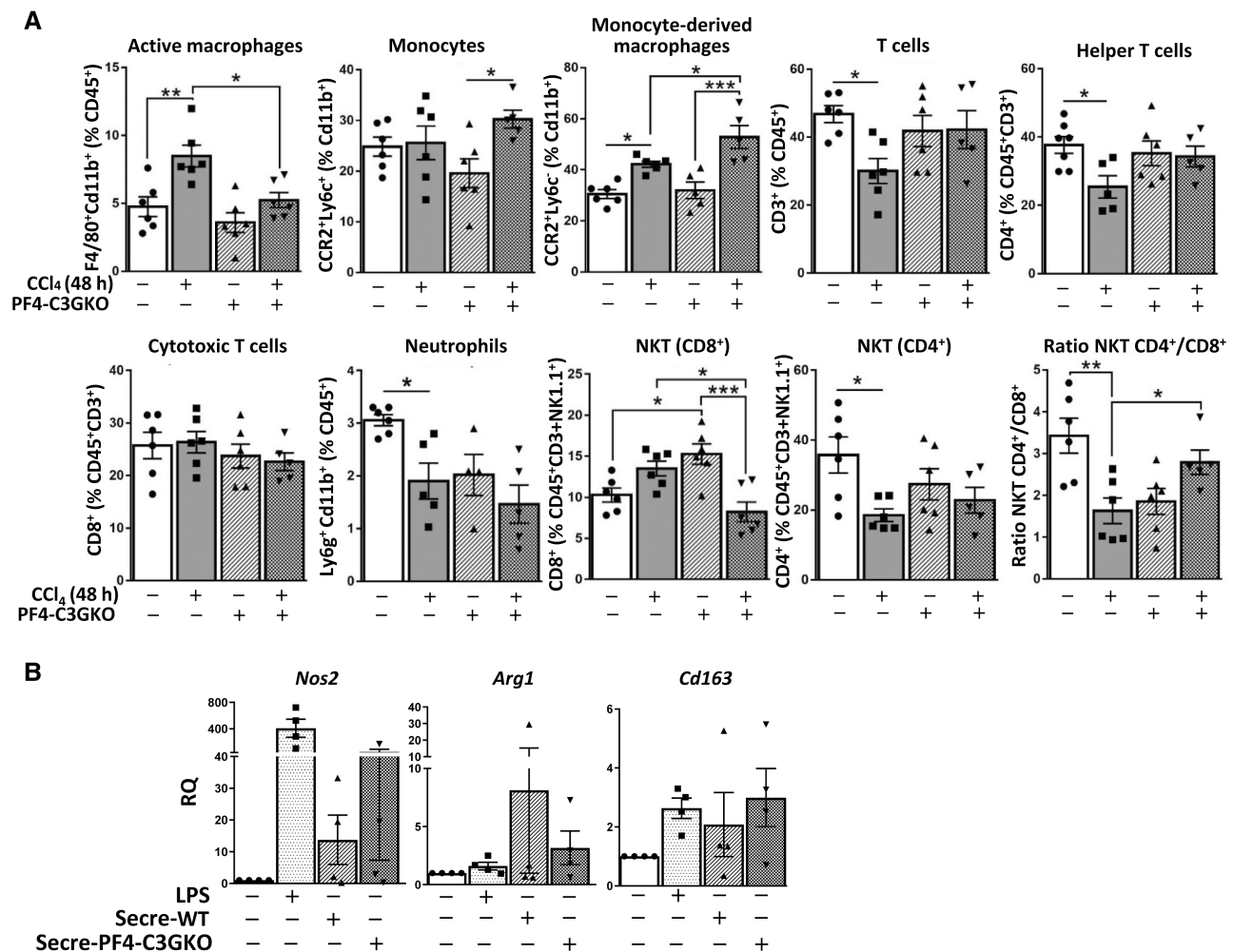


Figure 3. Platelet C3G regulates early liver immune response induced by CCl₄ and macrophage phenotype. (A) Mice lacking C3G (PF4-C3GKO) in megakaryocytes and platelets and their corresponding WT counterparts were treated with CCl₄ or vehicle (controls) for 48 h. Isolated nonparenchymal liver cells were analyzed by flow cytometry to determine the proportion of different immune cells. Histograms show the percentage (mean values \pm SEM) of the different subpopulations of CD45⁺ cells labelled as indicated. $n = 4-7$. * $p \leq 0.05$, ** $p \leq 0.01$, and *** $p \leq 0.001$ compared as indicated ($n = 4-8$). Scale bars: 20 μ m. (B) RT-qPCR analysis of *Nos2*, *Arg1*, and *Cd163* mRNA levels in macrophages treated with LPS, or secretomes from activated WT and PF4-C3GKO platelets. Histograms showing relative quantification (RQ) mean values \pm SEM and individual values of each sample ($n = 4$).

induced visible liver tumors after 14 weeks of treatment in both WT and PF4-C3GKO mice (Figure 4B and supplementary material, Table S3). However, despite the lower fibrosis observed at 8 weeks in WT animals, the number of WT mice bearing more tumors was higher than in PF4-C3GKO animals (Figure 4C), and tumors were larger (Figure 4D) and less differentiated (according to their higher *Afp* expression (Figure 4E).

Next, liver platelets were quantified. A significant increase in response to CCl₄ and DEN+CCl₄ was found only in WT mice at 8 and 14 weeks, especially in CCl₄ treatment (Figures 2C and 4F). However, no changes were detected upon DEN treatment.

The expression of CLD regulatory factors was also studied. The mRNA levels of *Cxcl4*, a chemokine important in fibrosis [43], increased in livers from WT and PF4-C3GKO mice treated with DEN+CCl₄ for 8 weeks, but differences were only significant in WT animals, probably because of the higher basal levels found in PF4-C3GKO livers (Figure 4G). Curiously, at 14 weeks,

Cxcl4 mRNA expression decreased in PF4-C3GKO livers in response to all treatments, whereas it increased in WT animals, being significantly higher in WT mice treated with CCl₄ or DEN+CCl₄. On the other hand, *Cxcl7* mRNA levels only increased in livers from PF4-C3GKO mice upon treatment with DEN+CCl₄ (8 or 14 weeks) or DEN for 14 weeks (Figure 4G). *Ccl2* mRNA levels were also increased in livers from PF4-C3GKO mice treated with DEN+CCl₄ for 8 weeks compared to WT animals (Figure 4G), while the opposite was observed at 14 weeks.

Moreover, *Hgf* mRNA levels decreased in the liver of WT mice treated with DEN+CCl₄ for 8 weeks but increased in PF4-C3GKO livers, being significantly higher than in WT animals (supplementary material, Figure S9A). Additionally, *Tgfb1* mRNA levels decreased in livers from WT mice in response to all treatments (supplementary material, Figure S9), remaining lower and unchanged in untreated PF4-C3GKO animals. No major changes in *Hgf* or *Tgfb1* mRNA levels were found after DEN+CCl₄

treatment for 14 weeks, and *Il6* mRNA expression remained unchanged under all conditions (supplementary material, Figure S9A).

Considering all this, we can highlight that the fibrosis degree is not directly associated with the presence of fewer tumors of reduced size in PF4-C3GKO mice.

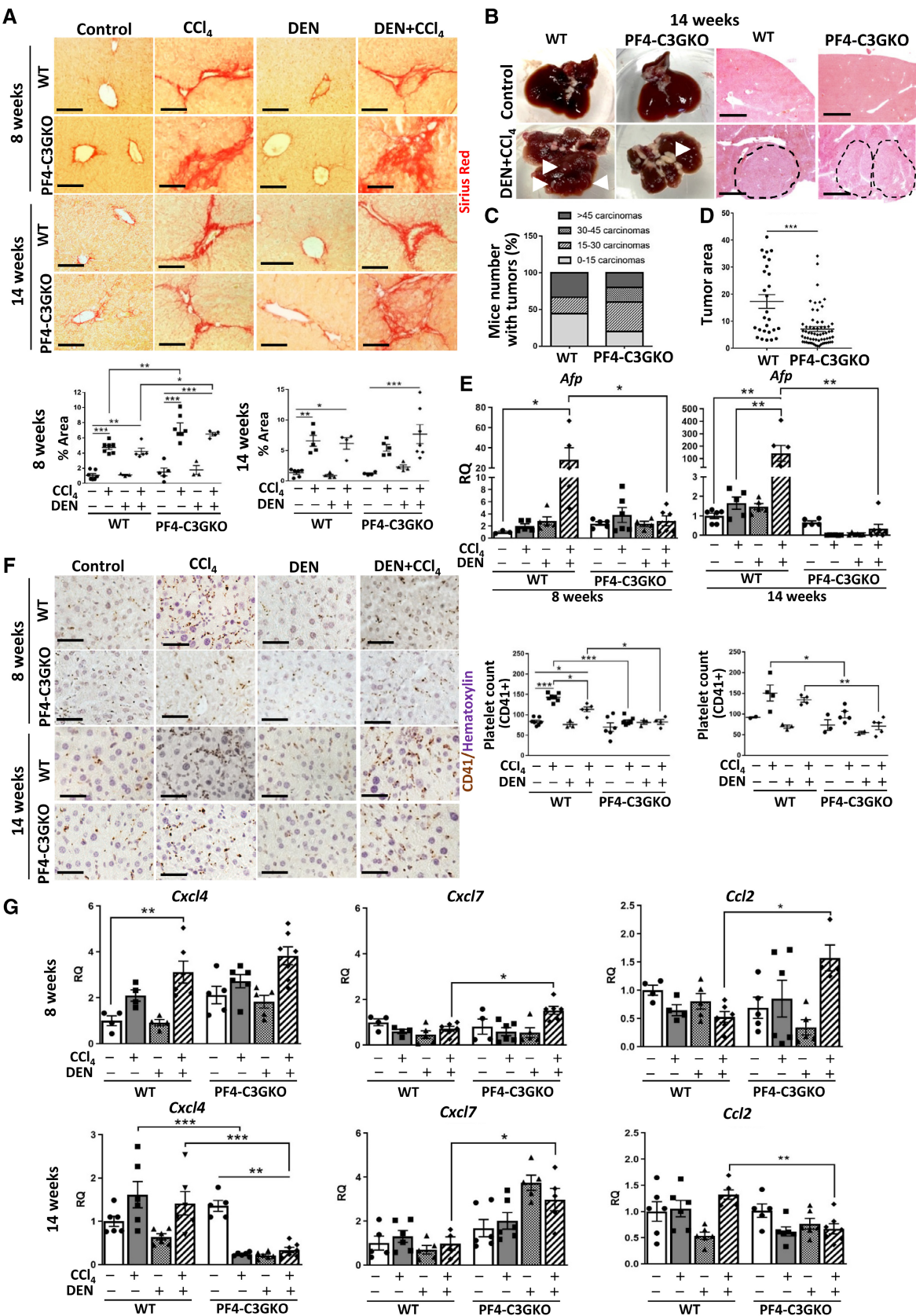


Figure 4 Legend on next page.

The different patterns of *Cxcl4*, *Cxcl7*, and *Ccl2* expression may explain the differences in fibrosis and tumor growth.

Liver immune response is modified by the absence of C3G in platelets in a model of hepatocarcinoma induced by DEN plus CCl₄

The differences in chemokines' expression in livers from WT and PF4-C3GKO mice induced by DEN+CCl₄ could modulate the immune response during HCC development/progression. Therefore, different immune cell populations were analyzed in liver tissues.

Figure 5A shows a significant increase in the number of liver macrophages (F4/80⁺ cells) in response to CCl₄ and DEN+CCl₄ at 8 weeks in both WT and PF4-C3GKO mice. However, while there were more macrophages in livers from WT animals treated with CCl₄, upon DEN+CCl₄ treatment more macrophages were detected in PF4-C3GKO livers. After 14 weeks of treatment, a tendency toward decreased liver macrophages in DEN- and DEN+CCl₄-treated WT mice was observed, while they increased in DEN+CCl₄-treated PF4-C3GKO mice. Moreover, the mRNA expression of the pro-inflammatory phenotype marker, *Nos2*, diminished in livers from WT mice treated with DEN+CCl₄ for 8 weeks, while remaining unaltered but significantly higher in the livers of PF4-C3GKO mice (Figure 5B). The mRNA levels of another marker of pro-inflammatory macrophages, *Cd68*, increased in PF4-C3GKO mouse livers treated with DEN+CCl₄ for 8 weeks, reaching significantly higher levels than in WT animals. Accordingly, the marker of protumor macrophages, *Cd163*, decreased (supplementary material, Figure S9B).

On the other hand, positive cells for CD11b (highly expressed in monocytes/monocyte-derived macrophages) tended to increase in livers from WT animals treated with CCl₄ for 8 weeks and in livers from PF4-C3GKO mice treated with DEN+CCl₄, reaching significantly higher levels than in WT animals (Figure 5C). In contrast, after 14 weeks of treatment, CD11b⁺ cells significantly increased in livers from WT mice treated with either CCl₄ or DEN+CCl₄, reaching higher levels than in PF4-C3GKO mice. Curiously, CD11b⁺ liver cells decreased upon DEN treatment in both WT and PF4-C3GKO mice at 8 and 14 weeks.

Liver cells positive for Ly6G (highly expressed in mature/activated neutrophils) showed a different pattern than that of CD11b⁺ cells. CCl₄ treatment induced an increase in Ly6G⁺ area in livers from WT animals at 8 and 14 weeks, but in PF4-C3GKO mice only at 14 weeks (Figure 5D). In contrast, upon DEN+CCl₄ treatment for 8 weeks, Ly6G⁺ area increased only in livers from PF4-C3GKO mice, and the opposite was observed at 14 weeks, whereas DEN treatment had no effect.

All these data indicate that mice lacking platelet C3G have a different inflammatory response to chronic CCl₄ treatment, which is more remarkable upon DEN+CCl₄ treatment. Notably, the number of macrophages (likely pro-inflammatory) is higher in PF4-C3GKO than in WT mice livers under this treatment.

Platelet proteomic profile is differentially regulated in mice lacking platelet C3G treated with DEN plus CCl₄

According to the literature [14,15], proteins differentially present in platelets from WT and PF4-C3GKO mice could be involved in the regulation of liver immune cells in CLD, controlling fibrosis and/or HCC development upon secretion. Therefore, we performed a wide proteomic analysis in PRP from untreated and DEN+CCl₄-treated mice at 14 weeks.

A total of 48 proteins were differentially present in PRPs from untreated PF4-C3GKO versus WT and 177 proteins in DEN+CCl₄ treated mice, 11 in common to both conditions (supplementary material, Figure S10A). Functional enrichment analyses (GO and Kyoto Encyclopedia of Genes and Genomes databases) of identified up- and/or downregulated proteins in PRPs from untreated or DEN+CCl₄-treated PF4-C3GKO versus WT mice (supplementary material, Figures S10B–E and S11A–C) revealed their involvement in different biological functions. Among them, in PRPs from untreated PF4-C3GKO mice the upregulation of proteins acting in stress response, catabolic processes, motility, defense response, endocytosis, proteolysis regulation, inflammatory response, and actin filament polymerization pathways is remarkable. Immune system proteins were downregulated in these PRPs (supplementary material, Figure S10B). In addition, in PRPs from DEN+CCl₄-treated PF4-C3GKO

Figure 4. Platelet C3G protects from fibrosis while favoring liver tumor growth. Mice lacking C3G (PF4-C3GKO) in megakaryocytes and platelets and their corresponding WT counterparts were treated with CCl₄, DEN, DEN+CCl₄, or vehicle (control) for indicated times (8 or 14 weeks). (A) Analysis of collagen accumulation assessed using Sirius Red staining in liver sections. Upper panels: representative microscope images; lower panels: graphics showing quantification of positive areas (percentage) for each sample and mean values ± SEM. (B) Macroscopic (left panels) and microscopic H&E (right panels) images of liver tumors induced by DEN+CCl₄ treatment and their corresponding controls. (C) Histograms showing percentage of mice (mean values ± SEM) with indicated number of tumors. (D) Graphic showing area (mean values ± SEM) occupied by tumors. (E) RT-qPCR analysis of *Afp* mRNA levels in liver samples. Histograms showing relative quantification (RQ) mean values ± SEM and the individual values of each sample after 8 (left panel) or 14 weeks (right panel) of treatment. (F) Immunohistochemical analysis of liver platelets detected with anti-CD41 antibody. Left panels: representative microscope images; right panels: graphics showing number of CD41-positive cells for each condition and mean values ± SEM. **p* ≤ 0.05, ***p* ≤ 0.01, and ****p* ≤ 0.001 compared as indicated (*n* = 4–8). Scale bars: 20 μm. (G) RT-qPCR analysis of *Cxcl4*, *Cxcl7*, and *Ccl2* mRNA levels in liver samples. Histograms showing RQ mean values ± SEM and individual values of each sample after 8 (upper panel) or 14 weeks (lower panel) of treatment. **p* ≤ 0.05, ***p* ≤ 0.01, and ****p* ≤ 0.001 compared as indicated (*n* = 4–8). Scale bars: 20 μm.

mice versus WT, an upregulation of proteins involved in response to stimulus, chemicals and stress, and metabolic processes was observed. A downregulation of proteins from

the immune system, inorganic substance, acute phase and inflammatory response, or wounding regulation pathways was also found in PRPs from DEN+CCl₄-treated

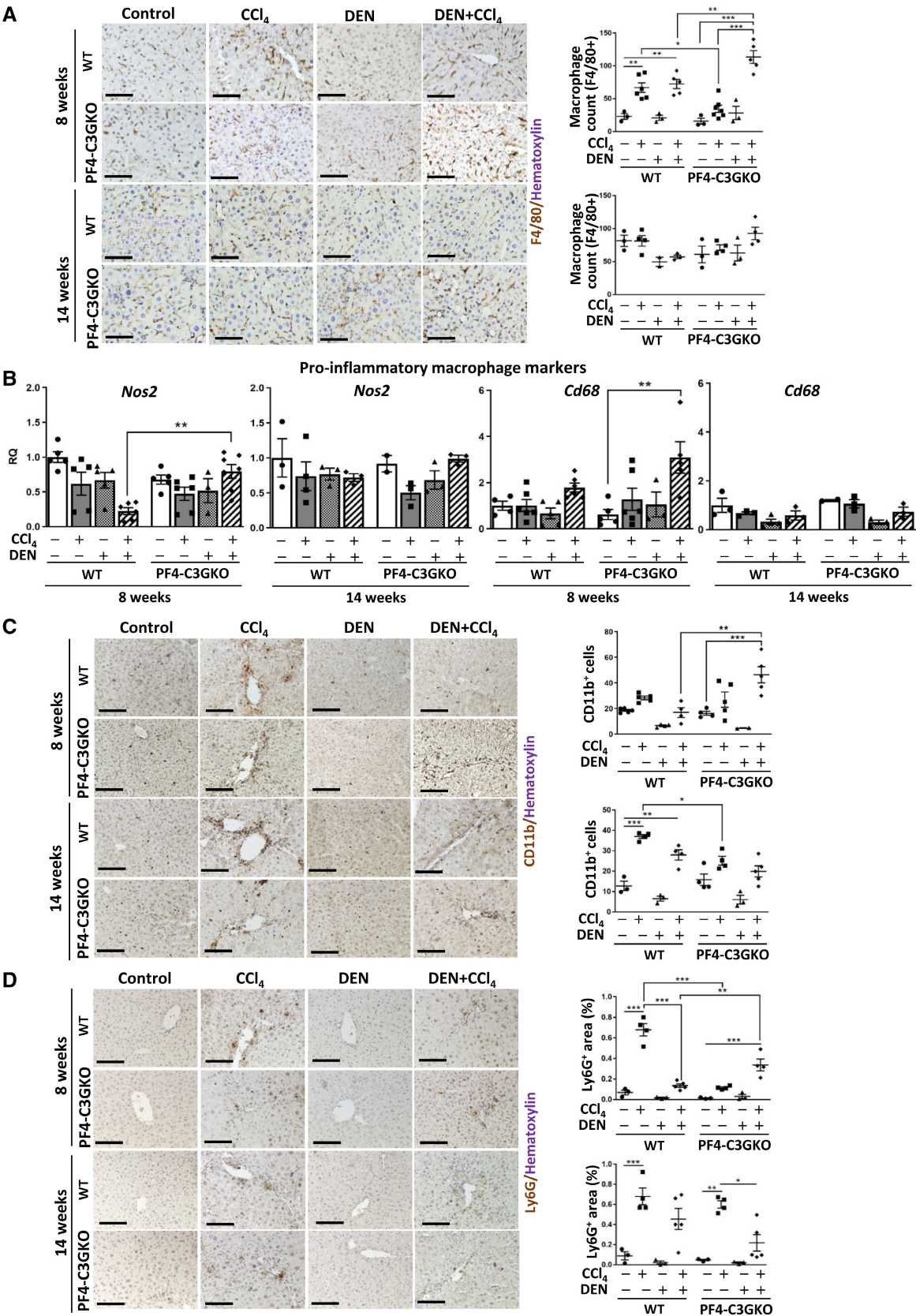


Figure 5 Legend on next page.

PF4-C3GKO mice compared to WT (supplementary material, Figure S10C). Additional analyses pointed to the regulation of more specific functional pathways such as platelet activation, adhesion, and aggregation (supplementary material, Figure S11A–C), functions previously shown to be regulated by C3G [32,34]. This confirms the validity of this study. We also found proteins implicated in integrin signaling, actin cytoskeleton regulation, cell migration, or immune response, among other processes regulated by C3G-Rap1 [34].

Among the proteins differentially present in PRPs from PF4-C3GKO versus WT mice treated with DEN+CCl₄, we found upregulation of Rap1a/b, GPV, CXCL4, α 2 and β 1 integrin, LECT2, Syntaxin 17, Rasa3, IGF1, Serpin b1, Arg1, BMP1, CXCL7, or Thbs1 (Figure 6A,B and supplementary material, Figure S12A,B). Others were downregulated such as IGFBP2, Syntaxin 11 (Stx11), Ngp, Saa2, Fibulin 5, Serpin 1c, SOD1, Fibronectin, or SOD3. In PRPs from untreated PF4-C3GKO versus WT mice (supplementary material, Figure S12A,B), examples of proteins upregulated were Slamf1, Rack1, VASP, Serpin1c, Ngp, Saa2, Snap23, and Cdc42, while among those downregulated were Collagen A1, Pleckstrin1, Serpin3k, Rasgrp2 (also named CALDAG-GEFI), L-selectin, α 6 integrin, AFP, GP1bb, and CD177.

CXCL7, GPV, and Stx11 protein levels were analyzed by western blotting in platelets to validate the wide proteomic analysis (Figure 6C). GPV and CXCL7 levels were higher in PF4-C3GKO than in WT platelets from untreated or treated mice with CCl₄, DEN, or DEN+CCl₄. On the other hand, Stx11 levels were downregulated in platelets from PF4-C3GKO mice treated with DEN or DEN+CCl₄ compared to WT platelets. These results validate data from wide proteomic analysis.

Some of the proteins differentially regulated in PRPs from DEN+CCl₄-treated PF4-C3GKO mice might play a role regulating liver cancer growth and/or fibrosis, although other proteins secreted by platelets could also be relevant. For example, CD40L, released by ADP-activated platelets, has recently been revealed as an antitumor signal in liver diseases [44]. Hence, we determined its levels in the secretome of WT and PF4-C3GKO platelets stimulated with ADP. Figure 6D shows a tendency to increase CD40L release by PF4-C3GKO compared to WT platelets. Therefore, it could contribute to decreasing liver tumor growth.

Discussion

Platelets are key players in CLD, regulating fibrosis and liver cancer. However, their functions and the underlying mechanisms need to be further characterized since opposite roles for platelets have been described [14,44–46]. Hence, based on the relevance of C3G protein as a regulator of platelet activation, spreading, secretion, and other nonhemostatic functions [32–36], we have studied the role of platelet C3G in liver fibrosis and HCC associated with fibrosis in genetically modified mouse models. We describe here for the first time that platelet C3G promotes the recruitment of platelets to the liver in a context of fibrosis induced by CCl₄ or DEN+CCl₄ (Figures 1C and 4F), exerting a protective role. The lower platelet recruitment to the liver in PF4-C3GKO mice might be due to a lower adhesion, owing to reduced surface levels of P-selectin and activated integrin α IIb β 3 [32,34]. Moreover, actin polymerization alterations that prevent their spreading, favoring kiss-and-run exocytosis, could play a role [33]. It is also notable that both overexpression of full-length C3G and C3G Δ Cat increase liver platelets in the absence of treatment at 8 weeks (Figure 1C), suggesting that C3G acts through both GEF-dependent and GEF-independent mechanisms to facilitate platelet recruitment to the liver.

Platelets can exert both antifibrotic [15,47,48] or pro-fibrotic actions by secreting different regulatory factors through their interplay with liver and immune cells [13,43,49]. The higher expression of *Hgf* mRNA in the liver of untreated and CCl₄-treated WT compared to PF4-C3GKO mice after 8 weeks (supplementary material, Figure S5) could facilitate an antifibrotic response [16]. IL-6, whose levels increased more in livers from tgC3GFL mice than from tgC3G Δ Cat or PF4-C3GKO mice compared to their corresponding WT mice under these conditions (Figure 2A), might also contribute to restraining fibrosis, limiting the differentiation of cirrhotic macrophages [50]. Moreover, the increased expression of *Ccl2* mRNA induced by DEN+CCl₄ at 8 weeks in livers from PF4-C3GKO mice (Figure 4G) might enhance monocyte recruitment and differentiation into macrophages, in agreement with previous studies on CLD and patient data [51,52]. Thus, upon liver damage, liver cells (hepatocytes, KCs, and HSCs) and platelets [8] secrete CCL2, promoting the generation of pro-inflammatory/fibrogenic macrophages that can induce HSCs' transdifferentiation into myofibroblasts. Hence, CCL2 blockade improved liver fibrosis in mice [52]. Supporting this role

Figure 5. Effect of platelet C3G on liver immune cells upon chemically induced liver cancer associated with fibrosis. Mice lacking C3G (PF4-C3GKO) in megakaryocytes and platelets and their corresponding WT counterparts were treated with CCl₄, DEN, DEN+CCl₄, or vehicle (control) for indicated times (8 or 14 weeks). (A) Immunohistochemical analysis of liver macrophages detected with F4/80 antibody. Left panels: representative microscope images; right panels: graphics showing number of F4/80-positive cells for each condition and mean values \pm SEM. (B) RT-qPCR analysis of mRNA levels of markers of pro-inflammatory macrophages, *Nos2* and *Cd68*, in liver samples. Histograms showing relative quantification (RQ) mean values \pm SEM and individual values of each sample after 8 or 14 weeks of treatment as indicated. (C) Immunohistochemical analysis of CD11b-positive cells. Left panels: representative microscope images; right panels: graphics showing number of CD11b-positive cells/field for each condition and mean values \pm SEM. (D) Immunohistochemical analysis of Ly6G-positive cells. Left panels: representative microscope images; right panels: graphics showing Ly6G-positive area for each condition and mean values \pm SEM. * $p \leq 0.05$, ** $p \leq 0.01$, and *** $p \leq 0.001$ compared as indicated ($n = 4-8$). Scale bars: 20 μ m.

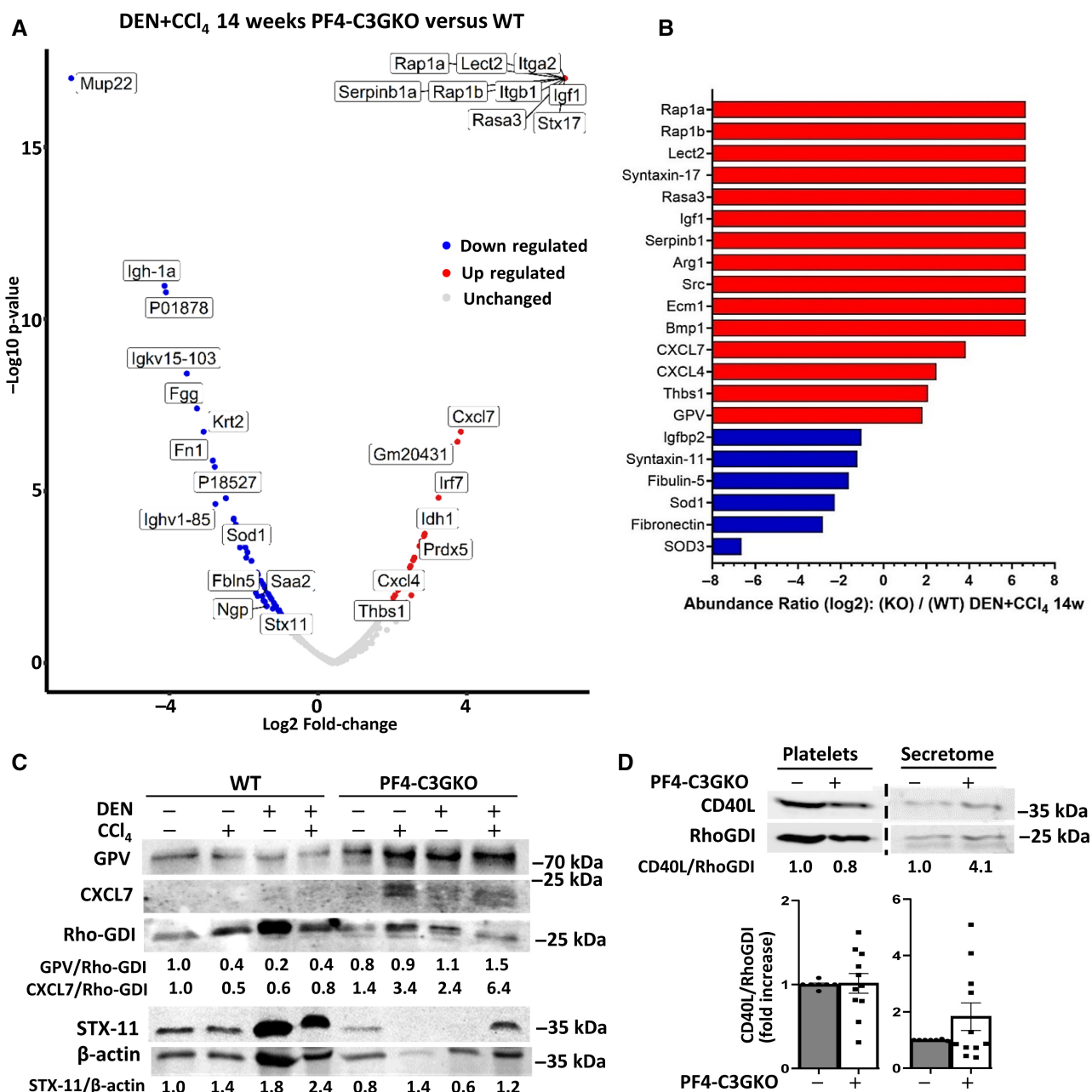


Figure 6. Deletion of C3G in platelets induces changes in proteins present in PRP upon chemically induced liver cancer associated with fibrosis. Mice lacking C3G (PF4-C3GKO) in megakaryocytes and platelets and their corresponding WT counterparts were treated with DEN +CCl₄ for 14 weeks. A wide proteomic analysis of PRP was performed, and then PRPs from PF4-C3GKO mice were compared with WT ones. (A) Volcano plot and (B) bar graphic showing proteins upregulated (red), downregulated (blue), or unchanged (gray) in PF4-C3GKO versus WT PRPs. The names of some proteins are included. The $-\log_{10}$ of p -value obtained from the applied statistical method is represented. (C) Western-blot analysis for GPV, CXCL7, and STX-11 protein levels normalized with Rho-GDI or β -actin in PRPs from mice treated with CCl₄, DEN, DEN+CCl₄, or vehicle (control) for 14 weeks. Quantification of band intensity versus Rho-GDI is shown. (D) Western blot analysis for CD40L in platelets and platelet secretome after activation of platelets with ADP normalized with Rho-GDI. Upper panels: representative western blots of WT and PF4-C3GKO samples. Membrane was cut, as indicated by dashed line. Lower panel: histograms show levels of CD40L in platelets and in secretomes (individual and mean values \pm SEM), expressed as fold increase of WT versus PF4-C3GKO values.

of CCL2 in PF4-C3GKO mice, we found that thrombin-activated PF4-C3GKO platelets secreted more CCL2 than C3G transgenic platelets (supplementary material, Figure S12C). Additionally, immune cells could contribute to enhancing fibrosis. For example, the lower number of neutrophils present in the liver of untreated PF4-C3GKO mice (Figure 3A) might facilitate fibrosis as specific subtypes of neutrophils can degrade collagen [53].

Our data also suggest that C3G effects on fibrosis would be at least partially dependent on its GEF activity, as transgenic overexpression of C3G lacking the catalytic domain did not protect from fibrosis as it did C3GFL overexpression (Figure 1A,B). However, considering the increased liver fibrosis found in PF4-C3GKO mice treated with CCl₄ (8 weeks) compared to tgC3G Δ Cat animals, GEF-independent

mechanisms may contribute to the antifibrotic effect of platelet C3G.

CXCL4 (PF4) synthesized and secreted by platelets and cancer cells can also promote CCl₄-induced liver fibrosis in mice [43]. The tendency to increase *Cxcl4* mRNA levels in livers from PF4-C3GKO compared to WT mice treated with CCl₄ or DEN+CCl₄ for 8 weeks (Figure 4G) supports it. CXCL4 protein levels were also upregulated in platelets from PF4-C3GKO compared to WT mice treated with DEN+CCl₄ for 14 weeks (Figure 6A,B). Moreover, thrombin-activated C3GKO platelets secrete more CXCL4 than C3G transgenic platelets (supplementary material, Figure S12C).

Curiously, despite the higher fibrosis observed in mice lacking C3G in platelets, liver tumors were smaller (Figure 4B) and more differentiated (Figure 4E). The higher levels of IL-6 present in the liver of WT versus PF4-C3GKO mice after treatment with CCl₄ for 8 weeks could support it (Figure 2A), as persistent activation of IL-6 signaling pathway promotes tumor growth [54]. It is also worth mentioning that, although 90% of HCC cases develop in a context of CLD [2], specific somatic mutations occurring in hepatocyte premalignant lesions of patients with liver cirrhosis can promote liver regeneration rather than HCC [55]. In addition, during a regenerative response to chronic liver damage, premalignant nodules can be surrounded by fibrotic septa, limiting tumor cell dissemination [56]. Hence, collagen accumulation in the liver correlates with less and smaller tumors in some studies [57], as occurs in PF4-C3GKO mice treated with DEN+CCl₄. ECM stiffness also plays a role. Hence, a higher matrix stiffness promotes a stem-like phenotype that could favor HCC development [58].

Concerning platelet function in HCC, a high platelet count has been associated with poor prognosis of HCC patients [18,20]. Hence, antiplatelet therapy reduces HCC risk in patients with viral hepatitis [19,45] and HCC development in a chronic hepatitis B mouse model, while having no effect on chemically induced HCC [59]. Tumor-associated platelets can protect HCC cells from immune cell recognition and by the release of their granule content facilitate their proliferation and transendothelial migration [15,60]. Platelets also induce proliferation of liver sinusoidal endothelial cells and hepatocytes, liver regeneration, and immune cell recruitment [14]. Therefore, the presence of more platelets in livers from WT compared to PF4-C3GKO mice treated with DEN+CCl₄ would explain the increased size of liver tumors and the differences in liver immune cell populations. On this point, C3G regulates the selective secretion of components from platelet granules [33,35,36], promoting tumor growth and metastasis in lung cancer and melanoma mouse models. In this regard, Syntaxin 11, which is required for platelet secretion and extension [61] and interacts with C3G [33], is downregulated in PRPs from PF4-C3GKO mice treated with DEN+CCl₄ for 14 weeks (Figure 6A–C). This further supports the implication of C3G-regulated platelet secretion. In this line, the upregulation of CXCL7 protein in PRPs from PF4-C3GKO treated with DEN+CCl₄ for

14 weeks (Figure 6A–C) could result in its higher secretion, although different immune cells can also express CXCL7 [62]. In cholangiocarcinoma, its levels increase [63], promoting proliferation and invasion [64]. High CXCL7 levels are also associated with inflammation and poor prognosis in hepatoblastoma [65]. In contrast, lower *Cxcl7* mRNA levels were detected in HCC [66]. In this study, the high levels of CXCL7 in PF4-C3GKO platelets and its high expression in livers from DEN+CCl₄-treated PF4-C3GKO mice do not correlate with HCC progression. Hence, CXCL7 could protect from HCC development/progression through regulation of immune cells.

On the other hand, the higher release of CD40L by PF4-C3GKO platelets stimulated with ADP (Figure 6D) could contribute to the antitumor effect based on the proved platelet-mediated enhancement of CD8 + T-cell-dependent antitumor immune response in MAFLD (formerly NAFLD) mouse models through P2Y12-induced CD40L release [44]. Hence, platelet C3G, through fine-tuning of the secretion of components from platelet granules, could regulate HCC by controlling the immune response. In this regard, the higher number of macrophages (likely pro-inflammatory) and CD11b⁺ cells (monocytes/monocyte-derived macrophages) (Figure 5C) in livers from PF4-C3GKO mice treated with DEN+CCl₄ for 8 weeks might facilitate an antitumor response by releasing pro-inflammatory and repair-associated cytokines [8]. In addition, changes in Ly6G⁺ population (likely neutrophils) upon DEN+CCl₄ treatment (Figure 5D) might play either a beneficial or deleterious role [67] depending on their subtype [68]: antitumoral N1 tumor-associated neutrophils (TANs) or protumor N2 TANs [67,69]. Hence, the larger Ly6G⁺ area detected in livers from WT compared to PF4-C3GKO mice treated with DEN+CCl₄ for 14 weeks and the higher *Ccl2* mRNA expression might support a higher presence of N2 TANs that might secrete CCL2, favoring tumor growth.

Platelet C3G could also regulate HCC and fibrosis through LECT2, whose expression is downregulated in HCC, favoring HCC development and the accumulation of immature inflammatory monocytes with immunosuppressive characteristics [70]. LECT2 can also enhance fibrosis [71]. Therefore, LECT2 upregulation in PRPs from DEN+CCl₄-treated PF4-C3GKO mice could reduce HCC development while increasing fibrosis.

In conclusion, in this work we have revealed a new function of the protein C3G from platelets in a model of liver fibrosis and HCC associated with fibrosis. While platelet C3G protects against fibrosis, it accelerates HCC development and/or progression (see schematic in supplementary material, Figure S13). All this might be mediated by changes in the liver inflammatory response (supplementary material, Tables S4 and S5) and the expression of growth factors, cytokines, and chemokines dependent on platelet C3G.

Acknowledgements

We thank M^a Luisa Hernáez from Universidad Complutense de Madrid (UCM) Proteomics Unit for

her very helpful assistance in the analysis of proteomic data. This work was supported by grants from the Spanish Ministry of Economy and Competitiveness and Science, Innovation and Universities (PID2022-137717OB-C21 to AP/AMC; PID2019-104143RB-C22 to AP; PID2022-137717OB-C22 to CG; PID2019-104143RB-C21 to CG; PID2019-104991RB-I00 and PID2022-136959OB-I00 to PB, PID2020-117650RA-I00 and CNS2023-144109 to AG-U, PID-2021-122766OB-I00 to AVM and funded by MICIU/AEI/10.13039/501100011033). All funding was cosponsored by the European 'ERDF A way of making Europe'. CB was supported by Grant PID2019-104143RB-C22. NP was a recipient of a Formacion de Profesorado Universitario fellowship from the Spanish Ministry of Education. MI is supported by a predoctoral contract from Comunidad de Madrid. MC is a recipient of a predoctoral contract from UCM.

Author contributions statement

CB, MI-G, NP, CF-I, PV, MC-R and JM were involved in methodology, data acquisition, analysis and/or interpretation. MR-F, CS and SM contributed to data analysis and reviewed the manuscript. SC obtained and analyzed proteomic data. AMC was involved in data acquisition, supervision and discussion of the results. AMV, AMC, AG-U, PB, CG and AP acquired funding. AP and PB conceived and designed the study and supervised the experiments. AP wrote the original draft of the manuscript. PB, CG and AG-U were involved in supervision, discussion of results and critically reviewing the manuscript. All authors read and approved the final manuscript.

Data availability statement

The data that support the findings of this study are openly available in the PRIDE database at <http://www.ebi.ac.uk/pride>, [72] 10.6019/PXD050819.

References

- Delgado ME, Cárdenas BI, Farran N, *et al*. Metabolic reprogramming of liver fibrosis. *Cells* 2021; **10**: 3604.
- Llovet JM, Kelley RK, Villanueva A, *et al*. Hepatocellular carcinoma. *Nat Rev Dis Primers* 2021; **7**: 6.
- Affo S, Yu L-X, Schwabe RF. The role of cancer-associated fibroblasts and fibrosis in liver cancer. *Annu Rev Pathol* 2017; **12**: 153–186.
- Sánchez PS, del Rígal MM, Djouder N. Inflammatory and non-inflammatory mechanisms controlling cirrhosis development. *Cancers (Basel)* 2021; **13**: 5045.
- Acharya P, Chouhan K, Weiskirchen S, *et al*. Cellular mechanisms of liver fibrosis. *Front Pharmacol* 2021; **12**: 671640.
- Kuwahara R, Kofman AV, Landis CS, *et al*. The hepatic stem cell niche: identification by label-retaining cell assay. *Hepatology* 2008; **47**: 1994–2002.
- Cuesta ÁM, Palao N, Bragado P, *et al*. New and old key players in liver cancer. *Int J Mol Sci* 2023; **24**: 17152.
- Triantafyllou E, Woollard KJ, McPhail MJW, *et al*. The role of monocytes and macrophages in acute and acute-on-chronic liver failure. *Front Immunol* 2018; **9**: 2948.
- Delgado A, Guddati AK. Clinical endpoints in oncology - a primer. *Am J Cancer Res* 2021; **11**: 1121–1131.
- Ramachandran P, Dobie R, Wilson-Kanamori JR, *et al*. Resolving the fibrotic niche of human liver cirrhosis at single-cell level. *Nature* 2019; **575**: 512–518.
- Cogliati B, Yashaswini CN, Wang S, *et al*. Friend or foe? The elusive role of hepatic stellate cells in liver cancer. *Nat Rev Gastroenterol Hepatol* 2023; **20**: 647–661.
- Hao X, Sun G, Zhang Y, *et al*. Targeting immune cells in the tumor microenvironment of HCC: new opportunities and challenges. *Front Cell Dev Biol* 2021; **9**: 775462.
- Malehmir M, Pfister D, Gallage S, *et al*. Platelet GPIb α is a mediator and potential interventional target for NASH and subsequent liver cancer. *Nat Med* 2019; **25**: 641–655.
- Pavlovic N, Rani B, Gerwins P, *et al*. Platelets as key factors in hepatocellular carcinoma. *Cancers (Basel)* 2019; **11**: 1022.
- Mussbacher M, Brunnthaler L, Panhuber A, *et al*. Till death do us part—the multifaceted role of platelets in liver diseases. *Int J Mol Sci* 2021; **22**: 3113.
- Murata S, Maruyama T, Nowatari T, *et al*. Signal transduction of platelet-induced liver regeneration and decrease of liver fibrosis. *Int J Mol Sci* 2014; **15**: 5412–5425.
- Li S, Lu Z, Wu S, *et al*. The dynamic role of platelets in cancer progression and their therapeutic implications. *Nat Rev Cancer* 2024; **24**: 72–87.
- Liu P, Hsu C, Su C, *et al*. Thrombocytosis is associated with worse survival in patients with hepatocellular carcinoma. *Liver Int* 2020; **40**: 2522–2534.
- Simon TG, Duberg A-S, Aleman S, *et al*. Association of Aspirin with hepatocellular carcinoma and liver-related mortality. *N Engl J Med* 2020; **382**: 1018–1028.
- Scheiner B, Kirstein M, Popp S, *et al*. Association of platelet count and mean platelet volume with overall survival in patients with cirrhosis and unresectable hepatocellular carcinoma. *Liver Cancer* 2019; **8**: 203–217.
- Maia V, Sanz M, Gutierrez-Berzal J, *et al*. C3G silencing enhances STI-571-induced apoptosis in CML cells through p38 MAPK activation, but it antagonizes STI-571 inhibitory effect on survival. *Cell Signal* 2009; **21**: 1229–1235.
- Gutiérrez-Uzquiza Á, Arechederra M, Molina I, *et al*. C3G down-regulates p38 MAPK activity in response to stress by Rap-1 independent mechanisms: involvement in cell death. *Cell Signal* 2010; **22**: 533–542.
- Priego N, Arechederra M, Sequera C, *et al*. C3G knock-down enhances migration and invasion by increasing Rap1-mediated p38 α activation, while it impairs tumor growth through p38 α -independent mechanisms. *Oncotarget* 2016; **7**: 45060–45078.
- Palao N, Sequera C, Cuesta ÁM, *et al*. C3G down-regulation enhances pro-migratory and stemness properties of oval cells by promoting an epithelial-mesenchymal-like process. *Int J Biol Sci* 2022; **18**: 5873–5884.
- Guerrero C, Fernandez-Medarde A, Rojas J, *et al*. Transformation suppressor activity of C3G is independent of its CDC25-homology domain. *Oncogene* 1998; **16**: 613–624.
- Martín-Encabo S, Santos E, Guerrero C. C3G mediated suppression of malignant transformation involves activation of PP2A phosphatases at the subcortical actin cytoskeleton. *Exp Cell Res* 2007; **313**: 3881–3891.
- Carabias A, Gómez-Hernández M, de Cima S, *et al*. Mechanisms of autoregulation of C3G, activator of the GTPase Rap1, and its catalytic deregulation in lymphomas. *Sci Signal* 2020; **13**: eabb7075.

28. Gutiérrez-Berzal J, Castellano E, Martín-Encabo S, et al. Characterization of p87C3G, a novel, truncated C3G isoform that is overexpressed in chronic myeloid leukemia and interacts with Bcr-Abl. *Exp Cell Res* 2006; **312**: 938–948.
29. Manzano S, Gutierrez-Uzquiza A, Bragado P, et al. C3G downregulation induces the acquisition of a mesenchymal phenotype that enhances aggressiveness of glioblastoma cells. *Cell Death Dis* 2021; **12**: 348.
30. Sequera C, Bragado P, Manzano S, et al. C3G is upregulated in hepatocarcinoma, contributing to tumor growth and progression and to HGF/MET pathway activation. *Cancers (Basel)* 2020; **12**: 1–22.
31. Ortiz-Rivero S, Baquero C, Hernández-Cano L, et al. C3G, through its GEF activity, induces megakaryocytic differentiation and proplatelet formation. *Cell Commun Signal* 2018; **16**: 101.
32. Gutiérrez-Herrero S, Maia V, Gutiérrez-Berzal J, et al. C3G transgenic mouse models with specific expression in platelets reveal a new role for C3G in platelet clotting through its GEF activity. *Biochim Biophys Acta, Mol Cell Res* 2012; **1823**: 1366–1377.
33. Fernández-Infante C, Hernández-Cano L, Herranz Ó, et al. Platelet C3G: a key player in vesicle exocytosis, spreading and clot retraction. *Cell Mol Life Sci* 2014; **311**: 84.
34. Gutiérrez-Herrero S, Fernández-Infante C, Hernández-Cano L, et al. C3G contributes to platelet activation and aggregation by regulating major signaling pathways. *Signal Transduct Target Ther* 2020; **5**: 29.
35. Hernández-Cano L, Fernández-Infante C, Herranz Ó, et al. New functions of C3G in platelet biology: contribution to ischemia-induced angiogenesis, tumor metastasis and TPO clearance. *Front Cell Dev Biol* 2022; **10**: 1026287.
36. Martín-Granado V, Ortiz-Rivero S, Carmona R, et al. C3G promotes a selective release of angiogenic factors from activated mouse platelets to regulate angiogenesis and tumor metastasis. *Oncotarget* 2017; **8**: 110994–111011.
37. Paquet KJ, Kamphausen U. The carbon-tetrachloride-hepatotoxicity as a model of liver damage. First report: long-time biochemical changes. *Acta Hepatogastroenterol (Stuttg)* 1975; **22**: 84–88.
38. Uehara T, Pogribny IP, Rusyn I. The DEN and CCl₄-induced mouse model of fibrosis and inflammation-associated hepatocellular carcinoma. *Curr Protoc Pharmacol* 2014; **66**: 14.30.1–14.30.10.
39. González-Rodríguez Á, Valdecantos MP, Rada P, et al. Dual role of protein tyrosine phosphatase 1B in the progression and reversion of non-alcoholic steatohepatitis. *Mol Metab* 2018; **7**: 132–146.
40. Brea R, Valdecantos P, Rada P, et al. Chronic treatment with acetaminophen protects against liver aging by targeting inflammation and oxidative stress. *Aging* 2021; **13**: 7800–7827.
41. Kolberg L, Raudvere U, Kuzmin I, et al. gprofiler2 -- an R package for gene list functional enrichment analysis and namespace conversion toolset gprofiler. *F1000Res* 2020; **9**: 709.
42. Pradere J-P, Kluwe J, De Minicis S, et al. Hepatic macrophages but not dendritic cells contribute to liver fibrosis by promoting the survival of activated hepatic stellate cells in mice. *Hepatology* 2013; **58**: 1461–1473.
43. Zaldivar MM, Pauels K, von Hundelshausen P, et al. CXC chemokine ligand 4 (Cxcl4) is a platelet-derived mediator of experimental liver fibrosis. *Hepatology* 2010; **51**: 1345–1353.
44. Ma C, Fu Q, Diggs LP, et al. Platelets control liver tumor growth through P2Y₁₂-dependent CD40L release in NAFLD. *Cancer Cell* 2022; **40**: 986–998.e5.
45. Lee M, Chung GE, Lee J, et al. Antiplatelet therapy and the risk of hepatocellular carcinoma in chronic hepatitis B patients on antiviral treatment. *Hepatology* 2017; **66**: 1556–1569.
46. Ramadori P, Klag T, Malek NP, et al. Platelets in chronic liver disease, from bench to bedside. *JHEP Rep* 2019; **1**: 448–459.
47. Takahashi K. Human platelets inhibit liver fibrosis in severe combined immunodeficiency mice. *World J Gastroenterol* 2013; **19**: 5250.
48. Ikeda N, Murata S, Maruyama T, et al. Platelet-derived adenosine 5'-triphosphate suppresses activation of human hepatic stellate cell: *in vitro* study. *Hepatol Res* 2012; **42**: 91–102.
49. Chauhan A, Adams DH, Watson SP, et al. Platelets: No longer bystanders in liver disease. *Hepatology* 2016; **64**: 1774–1784.
50. Buonomo EL, Mei S, Guinn SR, et al. Liver stromal cells restrict macrophage maturation and stromal IL-6 limits the differentiation of cirrhosis-linked macrophages. *J Hepatol* 2022; **76**: 1127–1137.
51. Karlmark KR, Weiskirchen R, Zimmermann HW, et al. Hepatic recruitment of the inflammatory Gr1⁺ monocyte subset upon liver injury promotes hepatic fibrosis. *Hepatology* 2009; **50**: 261–274.
52. Baeck C, Wei X, Bartneck M, et al. Pharmacological inhibition of the chemokine C-C motif chemokine ligand 2 (monocyte chemoattractant protein 1) accelerates liver fibrosis regression by suppressing Ly-6C⁺ macrophage infiltration in mice. *Hepatology* 2014; **59**: 1060–1072.
53. Saijou E, Enomoto Y, Matsuda M, et al. Neutrophils alleviate fibrosis in the CCl₄-induced mouse chronic liver injury model. *Hepatol Commun* 2018; **2**: 703–717.
54. Schmidt-Arras D, Rose-John S. IL-6 pathway in the liver: from physiopathology to therapy. *J Hepatol* 2016; **64**: 1403–1415.
55. Zhu M, Lu T, Jia Y, et al. Somatic mutations increase hepatic clonal fitness and regeneration in chronic liver disease. *Cell* 2019; **177**: 608–621.e12.
56. Bhattacharjee S, Hamberger F, Ravichandra A, et al. Tumor restriction by type I collagen opposes tumor-promoting effects of cancer-associated fibroblasts. *J Clin Invest* 2021; **131**: e146987.
57. Baglieri J, Zhang C, Liang S, et al. Nondegradable collagen increases liver fibrosis but not hepatocellular carcinoma in mice. *Am J Pathol* 2021; **191**: 1564–1579.
58. Wei J, Yao J, Yang C, et al. Heterogeneous matrix stiffness regulates the cancer stem-like cell phenotype in hepatocellular carcinoma. *J Transl Med* 2022; **20**: 555.
59. Sitia G, Aiolfi R, Di Lucia P, et al. Antiplatelet therapy prevents hepatocellular carcinoma and improves survival in a mouse model of chronic hepatitis B. *Proc Natl Acad Sci USA* 2012; **109**: E2165–E2172.
60. Tesfamariam B. Involvement of platelets in tumor cell metastasis. *Pharmacol Ther* 2016; **157**: 112–119.
61. Ye S, Karim ZA, Al Hawas R, et al. Syntaxin-11, but not syntaxin-2 or syntaxin-4, is required for platelet secretion. *Blood* 2012; **120**: 2484–2492.
62. Brown AJ, Sepuru KM, Sawant KV, et al. Platelet-derived chemokine CXCL7 dimer preferentially exists in the glycosaminoglycan-bound form: implications for neutrophil-platelet crosstalk. *Front Immunol* 2017; **8**: 1248.
63. Wu Q, Tu H, Li J. Multifaceted roles of chemokine C-X-C motif ligand 7 in inflammatory diseases and cancer. *Front Pharmacol* 2022; **13**: 914730.
64. Guo Q, Jian Z, Jia B, et al. CXCL7 promotes proliferation and invasion of cholangiocarcinoma cells. *Oncol Rep* 2017; **37**: 1114–1122.
65. Guo F, Ru Q, Zhang J, et al. Inflammation factors in hepatoblastoma and their clinical significance as diagnostic and prognostic biomarkers. *J Pediatr Surg* 2017; **52**: 1496–1502.
66. Zajkowska M, Mroczko B. Chemokines in primary liver cancer. *Int J Mol Sci* 2022; **23**: 8846.
67. Liu K, Wang F-S, Xu R. Neutrophils in liver diseases: pathogenesis and therapeutic targets. *Cell Mol Immunol* 2021; **18**: 38–44.
68. Xue R, Zhang Q, Cao Q, et al. Liver tumour immune microenvironment subtypes and neutrophil heterogeneity. *Nature* 2022; **612**: 141–147.

69. Finisguerra V, Di Conza G, Di Matteo M, *et al.* MET is required for the recruitment of anti-tumoural neutrophils. *Nature* 2015; **522**: 349–353.
70. L'Hermitte A, Pham S, Cadoux M, *et al.* Lect2 controls inflammatory monocytes to constrain the growth and progression of hepatocellular carcinoma. *Hepatology* 2019; **69**: 160–178.
71. Xu M, Xu H-H, Lin Y, *et al.* LECT2, a ligand for Tie1, plays a crucial role in liver fibrogenesis. *Cell* 2019; **178**: 1478–1492.e20.
72. Perez-Riverol Y, Bai J, Bandla C, *et al.* The PRIDE database resources in 2022: a hub for mass spectrometry-based proteomics evidences. *Nucleic Acids Res* 2022; **50**: D543–D552.

SUPPLEMENTARY MATERIAL ONLINE

Supplementary materials and methods

Figure S1. Effect of C3G overexpression in platelets on CCl₄-induced liver fibrosis.

Figure S2. Low-magnification images of collagen and α -SMA accumulation in the liver.

Figure S3. C3G deficiency in platelets increases liver damage after chronic treatment with CCl₄.

Figure S4. Regulation by platelet C3G of regulatory factors of fibrosis and inflammation.

Figure S5. Regulation of regulatory factors of fibrosis and inflammation by platelet C3G.

Figure S6. Quantification of liver IL-6, IL-1 β and CCL2 protein levels.

Figure S7. Quantification of liver IL-6, IL-1 β , and CCL2 protein levels.

Figure S8. Effect of platelet C3G on acute liver damage.

Figure S9. Impact of C3G deletion in platelets on regulatory factors of fibrosis and inflammation during chemically induced HCC associated with fibrosis.

Figure S10. C3G deletion in platelets induces changes in platelet protein profile under basal conditions and upon chemically induced HCC associated with fibrosis.

Figure S11. C3G deletion in platelets induces changes in platelet proteins involved in different biological processes in chemically induced HCC associated with fibrosis.

Figure S12. Deletion of C3G in platelets induces changes in proteins present in PRP upon chemically induced liver cancer associated with fibrosis.

Figure S13. Schematic showing predictive liver damage induced by CCl₄ and DEN+CCl₄ over time, with regulation by platelet C3G.

Table S1. Sequences of primers used for RT-qPCR analyses.

Table S2. Analysis of fibrosis using the METAVIR scoring system.

Table S3. Analysis of fibrosis using the METAVIR scoring system (WT and PF4-C3GKO mice).

Table S4. Effect of platelet C3G on changes in liver immune cell populations induced by treatment with CCl₄, DEN, and DEN+CCl₄ for 8 weeks.

Table S5. Effect of platelet C3G on changes in liver immune cell populations induced by treatment with CCl₄, DEN, and DEN+CCl₄ for 14 weeks.